Study on the Decomposition Pathways and Products of C_4F_7N/N_2

Li Haoyang, Fu Yuwei, Zheng Borui, Wang Xinxin, and Duan Jiandong

Abstract SF_6 has been widely used in electric industries due to its good insulation characteristics and arc extinguishing performance, but research on its substitutes has become a hot topic in recent years to reduce serious greenhouse effect caused by SF_6. Perfluoroisobutyronitrile (C_4F_7N) and its mixtures are promising to replace SF_6 due to their excellent insulation performance and relative low greenhouse effect. This article studied basic decomposition paths of C_4F_7N/N_2 gas mixtures using density functional theory (DFT), and calculated the main decomposition reaction rate constants with transition state theory (TST). The results can lay a theoretical basis for C_4F_7N gas insulated electrical equipment insulation evaluation.

Keywords Insulating gas · Decomposition mechanism · Density functional theory · SF_6 replacement

1 Introduction

SF_6 is recognized as a greenhouse gas that has a great harm to the atmospheric environment. Its greenhouse warming potential (GWP) is 23,900 times than that of CO_2, and its survival life in the atmosphere is 3400 years [1]. In the "Kyoto Protocol" signed in 1997, SF_6 was listed as one of the six restricted-use greenhouse gases, and the use of SF_6 was required to be restricted. Looking for alternative gas for SF_6 to tackle with environmental issues, has become a hot topic in recent decades [2]. Among the existing SF_6 replacements, perfluoroisobutyronitrile (C_4F_7N) and its mixtures have excellent insulation ability and arc extinguishing ability, and its global warming potential is relatively lower than SF_6 [3–6]. At present, most of the researches on C_4F_7N gas are from the perspective of insulation performance. Literature [7, 8] studied the power frequency breakdown voltage characteristics of C_4F_7N/CO_2 and C_4F_7N/N_2 mixed gas by building an insulation characteristic experimental platform, and the results show that the C_4F_7N mixed gas has the potential to be

L. Haoyang (✉) · F. Yuwei · Z. Borui · W. Xinxin · D. Jiandong
School of Electrical Engineering, Xi'an University of Technology, Xi'an 710048, China
e-mail: 491018862@qq.com

W. Ma et al. (eds.), *The Proceedings of the 9th Frontier Academic Forum of Electrical Engineering*, Lecture Notes in Electrical Engineering 742,
https://doi.org/10.1007/978-981-33-6606-0_15

applied to gas insulation equipment. GE company do arc extinguishing test by used C_4F_7N/CO_2 and SF_6 on 420 kV disconnector. Comparing the test results we can see The arcing time is slightly shorter than that of SF_6, which indicates that gas mixture's arc extinguishing performance is close to SF_6 [9]. Kieffel et al. observed there are many kinds of species in the decomposition products of C_4F_7N such as CF_3CN [10]. Zhang Xiaoxing team studied the decomposition characteristics of C_4F_7N/CO_2 gas mixture theoretically, then found that the main decomposition species are CF_3, F, CF, CNF and CN [11]. Literature [12–14] show C_4F_7N gas mixture is suitable for various types of High-voltage (HV) and Medium-voltage (MV) gas insulated equipment.

In this paper,the main decomposition pathways and formed species of C_4F_7N/N_2 mixture were investigated, and we used high level quantum chemistry calculations with density functional theory (DFT). There are five main pathways in the decomposition, two derefent reaction types are shown in this paper to explore the feasibility of C_4F_7N/N_2 mixture's application in insulation equipment.

2 Calculation Method

B3LYP functional form in the density functional theory [15] combined with the 6-311G (d, p) basis set [16–20] is used in this paper to study decomposition reactions of C_4F_7N/N_2 mixtures, and calculate the optimized geometric configuration and energy of the product. Based on above calculations, the rate constants of the reactions are calculated with transition state theory according to Formula (1).

$$K(T) = \frac{k_B T}{h} \frac{Q^{\neq}(T)}{\varphi^R(T)} e^{-V^{\neq}/k_B T} \tag{1}$$

where T is temperature; is Boltzmann's constant; h is the Planck's constant; and are the transition state structure and the internal partition functions of the reactants; is the potential energy difference between the transition state and the reactant.

3 Results and Discussion

The reactions involved in this paper include the combine of C_4F_7N molecules with N atoms and the decomposition reaction of $C_4F_7N_2$ molecules. The decomposition reaction channels mainly study the breaking reactions of C–C bonds, C–F bonds, and C–N bonds. First, we optimize the geometric configuration of C_4F_7N and N atoms to combine them. Optimized structure of some molecules, such as $C_4F_7N_2$, as shown in Fig. 1.

Table 1 lists the main decomposition reactions of $C_4F_7N_2$ molecules. The decomposition pathways of $C_4F_7N_2$ molecules include three barrierless reactions: B, D, and E, and two reactions A and C with transition states.

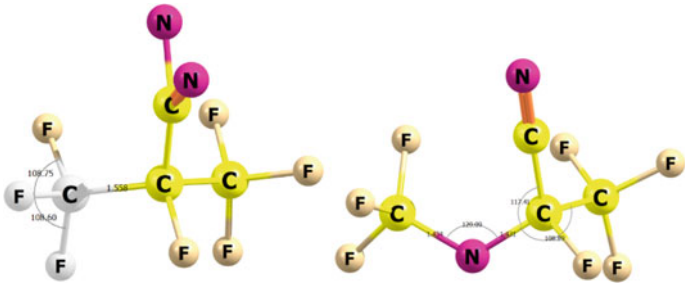

Fig. 1 Molecular geometry of $C_4F_7N_2$

Table 1 Main decomposition reactions of C_4F_7NO molecules

	Decomposition pathway		ΔE (kcal mol^{-1})
$C_4F_7N \xrightarrow{(+N)} C_4F_7N_2$(Geometry optimization)	*A*	$C_4F_7E_2 \longrightarrow C_3F_7 + CN_2$	85.341
	B	$C_4F_7N_2 \longrightarrow C_4F_6N_2 + F$	42.043
	C	$C_4F_7N_2 \longrightarrow C_3F_4N_2 + CF_3$	6.275
	D	$C_4F_7N_2 \longrightarrow C_3F_7N + CN$	39.533
	E	$C_4F_7N_2 \longrightarrow C_3F_4N + CF_3N$	57.731

3.1 Optimization of Geometric Configuration of Reaction Particles

This article shows reaction E without a transition state and reaction A with transition state TS1. Figures 2 and 3 show the optimized molecular structures and key geometric parameters in the reactions E and A, respectively.

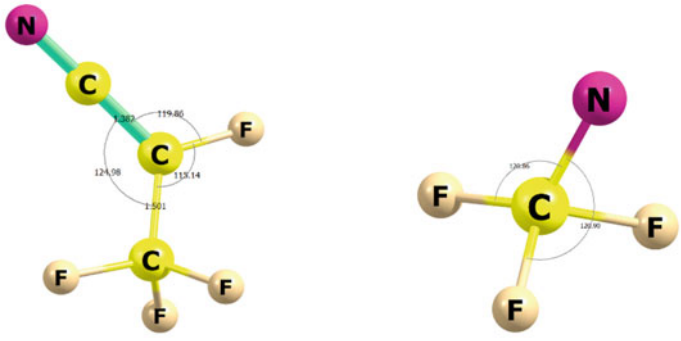

(a) C_3F_4N (b) CF_3N

Fig. 2 The geometry of the particles involved in reaction E

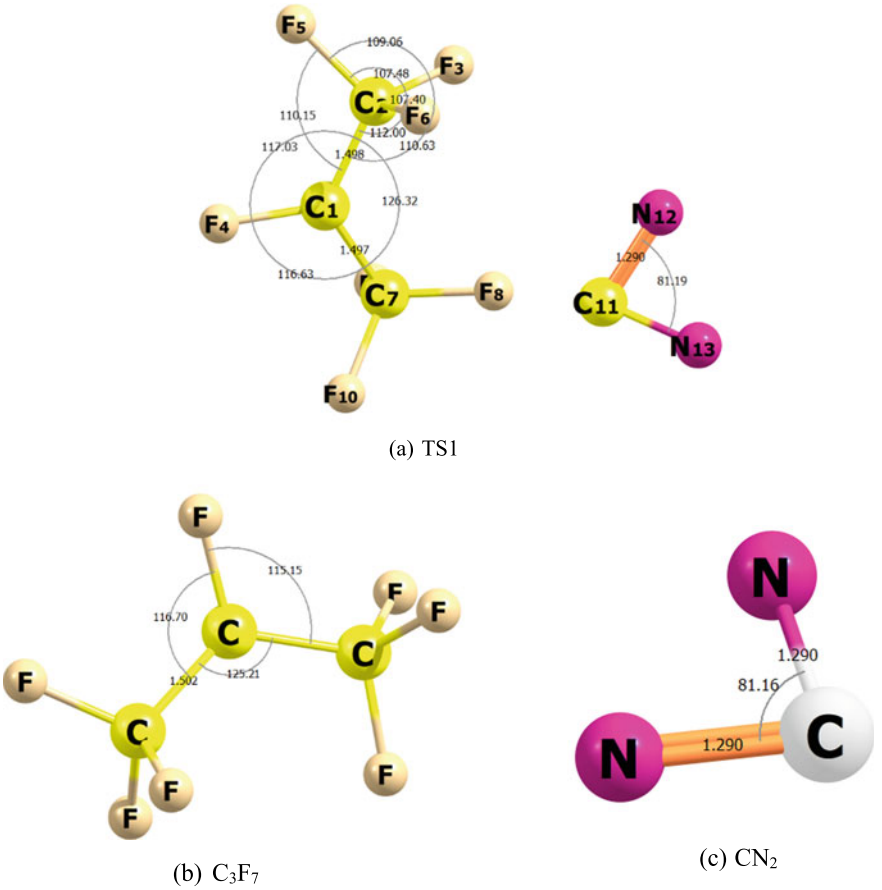

(a) TS1

(b) C_3F_7

(c) CN_2

Fig. 3 The geometry of the particles involved in reaction A

3.2 Particle Energy and Frequency Calculation

At the B3LYP/6-311G(d,p) level, the stable point energies of the decomposition reaction channels of the C–C, C–N and C–F of the $C_4F_7N_2$ molecular center carbon bonds were calculated, including reactants, transition states, intermediate products and the zero-point vibration energy (ZPE) and total energy of the product (including electronic energy and zero-point energy) E total show in Table 2.

The vibration frequencies of the particles involved in the reactions E and A calculated at the same calculation level are listed in Table 3.

Table 2 Energy information of reactants, transition states and products

R	Particle	*ZPE*/(Kcal/Mol)	E_{total}/(Hartree/Particle)
E	C_3F_4N	18.80470	−568.483449
	CF_3N	9.58045	−392.295517
A	TS1	26.97601	−960.759584
	C_3F_7	22.70776	−813.342736
	CN_2	5.37642	−147.457949

Table 3 Vibration frequencies of reactants, transition states and products calculated

R	Particle	Vibration frequencies/cm^{-1}
E	$C_4F_7N_2$	30.8478, 60.6705, 72.1769, 115.0043, 140.8293, 167.965, 244.0457, 244.0965, 294.7629, 314.3399, 336.0174, 372.8911, 394.0623, 499.6059, 504.7738, 533.4358, 552.3559, 574.3575, 619.4027, 713.2646, 728.7748, 766.2051, 987.4776, 1004.777, 1082.6901, 1160.8261, 1176.3056, 1204.0847, 1237.3946, 1252.2296, 1254.9442, 1301.426, 1766.1114
	C_3F_7N	24.3335, 143.4126, 153.4262, 245.8152, 379.805, 397.9495, 445.3487, 466.896, 567.7119, 581.4768, 647.9747, 761.7524, 1082.1913, 1150.5321, 1211.3964, 1352.4843, 1363.6814, 2177.8884
	CF_3N	281.0459, 322.6832, 537.1063, 564.9434, 596.7825, 884.6621, 969.2313, 1166.6748, 1378.4914
A	$C_4F_7N_2$	30.8478, 60.6705, 72.1769, 115.0043, 140.8293, 167.965, 244.0457, 244.0965, 294.7629, 314.3399, 336.0174, 372.8911, 394.0623, 499.6059, 504.7738, 533.4358, 552.3559, 574.3575, 619.4027, 713.2646, 728.7748, 766.2051, 987.4776, 1004.777, 1082.6901, 1160.8261, 1176.3056, 1204.0847, 1237.3946, 1252.2296, 1254.9442, 1301.426, 1766.1114
	TS1	−16.1303, 13.25, 18.5004, 22.0541, 28.0063, 35.8521, 43.2973, 48.9005, 68.152, 149.5413, 265.3851, 298.481, 321.0278, 344.3736, 433.3824, 462.355, 539.7261, 540.143, 583.1827, 606.1381, 611.5635, 697.5165, 699.5499, 764.5668, 989.3096, 1112.2135, 1147.1655, 1163.6724, 1190.8684, 1227.3115, 1361.7166, 1431.4409, 1651.3464
	C_3F_7	25.9352, 32.4459, 119.1742, 157.6536, 257.7729, 294.2606, 319.8556, 345.3579, 451.3748, 480.186, 535.3934, 543.0533, 606.7509, 632.4284, 697.508, 766.7246, 985.1657, 1118.4127, 1142.8962, 1173.2562, 1199.4602, 1231.7563, 1354.9063, 1412.5805
	CN_2	1008.835, 1136.8796, 1615.1434

3.3 Decomposition of C_4F_7N/N_2 Mixtures

Figure 4 shows the energy changes of all reaction pathways. Pathway A corresponds to the break of the C–C bond between the core carbon atom and the adjacent carbon atom in the $C_4F_7N_2$ molecule. This process forms the CN_2 and $F_3C(F)CF_3$. The energy difference between the reaction product and the reactant is 85.341 kcal · mol^{-1}, and in reaction A, there is a transition state TS1, and the reactant $C_4F_7N_2$

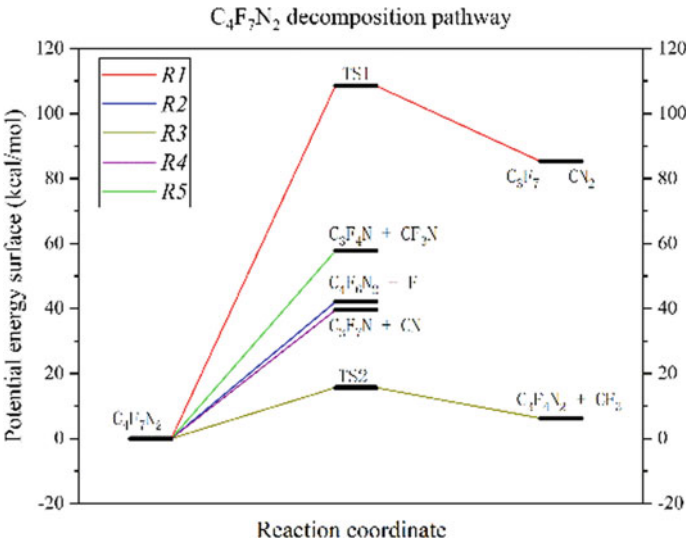

Fig. 4 The energy changes of all reaction pathways

needs to cross the energy barrier of 108.559 kcal · mol^{-1} to occur. Pathway B corresponds to the breaking process of C-F bond between carbon atom and F atom, and $F_2NC(FC{\equiv}F)CF_3$ molecule and F atom are formed. The reaction process needs to absorb 42.043 kcal · mol^{-1} energy. For pathway C also corresponds to the process of breaking the C–C bond between the central carbon atom of $C_4F_7N_2$ and the adjacent carbon atom. This process has the transition state TS2, and the energy potential barrier is 15.688 kcal · mol^{-1}. After crossing the barrier, the products $F_3CNC(F)CN$ and CF_3 were obtained, and the energy difference between the product and the reactant $C_4F_7N_2$ is only 6.275 kcal · mol^{-1}. Similarly, reaction D is a process in which the C–C bond between the central carbon atom and the adjacent carbon atom CN in $C_4F_7N_2$ is broken. This process absorbs 39.533 kcal · mol^{-1} energy to generate $F_3CC(F)NCF_3$ and CN. Pathway E shows the C-N bond breaking process between the central carbon atom of $C_4F_7N_2$ and the adjacent nitrogen atom, absorbing 57.731 kcal · mol^{-1} energy and generating $F_3CC(F)CN$ and F_3CN. Among the five reaction pathways, pathway A needs to absorb the energy of 85.341 kcal · mol^{-1}, which is the most difficult to occur, while pathway C only needs to absorb the energy of 6.275 kcal · mol^{-1}, which is the most prone process.

4 Conclusion

In this paper, the DFT-B3LYP/6-311G (d, p) method is used to calculate the decomposition reactions and main decomposition components of the $C_4F_7N_2$ molecule.There are five decomposition pathways shown in this paper such as A-E, and the main

decomposition species are CxFxNx, CxNx. Microscopic data such as the molecular structure, key geometric parameters, zero-point vibration energy and frequency are important to compute the composition of C_4F_7N plasma when C_4F_7N used in power equipment as an insulator. Therefore these parameters are the basis in any attempt to test the dielectric properties of C_4F_7N used in power equipments for insulating.

References

1. Xiao, Hanyan, Xiaoxing Zhang, and Song Xiao. 2017. Experiment of the influence of environmental media obstruct on the discharge degradation of SF6. *Journal of Electrical Technology* 20: 26–33.
2. Xiao, Dengming. 2016. Development prospect of gas insulation based on environmental protection. *High Voltage Engineering.*
3. Xianglian, Yan, Gao Keli, Yu. Zheng, Li. Zhibing, Wang Hao, He. Jie, and Liu Yan. 2008. Research progress of SF_6 mixed gas and alternative gas . *Power Grid Technology* 42 (06): 1837–1844.
4. Kieffel, Y., and F. Biquez. 2015. SF6 alternative development for high voltage switchgears. In *2015 IEEE Electrical Insulation Conference.* New York: IEEE.
5. xiaoxing, Zhang, Tian Shuangshuang, and Xiao Song, et al. 2018. SF6 review of alternative gas research. *Journal of Electrical Technology* (1): 2883–2893.
6. Wenjun, Zhou, Yu. Zheng, Yang Shuai, et al. 2016. Research progress and trend of environment-friendly insulating gas replacing SF6 . *High Voltage Appliances* 12: 8–14.
7. Xiaoxing, Zhang, Chen Qi, Zhang Ji, Li Yi, and Xiao Song. Environmental protection type C_4F_7N/CO_2 hybrid gas breakdown characteristics at high pressure. *Journal of Electrical Technology* 1–7.
8. Shizhuo, Hu, Zhou Wenjun, Zheng Yu, Yu Jianhui, Zhang Tiantian, and Wang Lingzhi. Mechanical frequency breakdown experiment and synergy analysis of C_4F_7N/CO_2 and C_4F_7N/N_2 hybrid gas. *High Voltage Technology* 1–10.
9. Kieffel, Y., François Biquez, and P. Ponchon. 2015. SF6 alternative development for high voltage switchgears. In *Electrical Insulation Conference.* New York: IEEE.
10. Kieffel, Y., T. Irwin, P. Ponchon, et al. 2016. Green gas to replace SF6 in electrical grids. *IEEE Power and Energy Magazine* 14 (2): 32–39.
11. Zhang, X., Y. Li, S. Xiao, S. Tian, and J. Tang. 2017. Theoretical study of the decomposition mechanism of environmentally friendly insulating medium C_3F_7CN in the presence of H_2O in a discharge. *Journal of Physics D: Applied Physics* 50 (32).
12. Preve, C., R. Maladen, and D. Piccoz. 2016. Method for validation of new eco-friendly insulating gases for medium voltage equipment. In Proceedings of the 2016 IEEE International Conference on Dielectric. ICD 2016, 2016, 235–240. https://doi.org/10.1109/ICD.2016.7547588.
13. Owens, J.G. 2016. Greenhouse gas emission reductions through use of a sustainable alternative to SF6. In *IEEE Electrical Insulation Conference (EIC)*, Montréal, Canada, 2016, 535–538.
14. Kieffel, Y. 2016. Characteristics of g3-an alternative to SF6. In *IEEE International Conference on Dielectrics (ICD)*, 2016, vol. 2, 880–884.
15. Stephens, P.J., F.J. Devlin, C.F. Chabalowski, and M.J. Frisch. 1994. Ab initio calculation of vibrational absorption and circular dichroism spectra using density functional force fields. *Journal of Physical Chemistry* 98 (45): 11623–11627.
16. Mclean, A.D., and G.S. Chandler. 1980. Contracted Gaussian basis sets for molecular calculations. I. Second row atoms, Z=11–18. *Journal of Chemical Physics* 72: 5639.
17. Wachters, A.J.H. 2003. Gaussian basis set for molecular wavefunctions containing third-row atoms. *Journal of Chemical Physics* 52 (3): 1033–1036.

18. Hay, P.J. 1977. Gaussian basis sets for molecular calculations—The representation of 3d orbitals in transition-metal atoms. *Journal of Chemical Physics* 66: 4377–4384.
19. Mcgrath, M.P., and L. Radom. 1991. Extension of Gaussian-1 (G1) theory to bromine-containing molecules. *Journal of Chemical Physics* 94 (1): 511–516.
20. Tang, Ju., Yang Dong, Zeng Fuping, and Zhang Xiaoxing. 2016. Research status of insulation fault diagnosis method and technology of SF6 equipment based on decomposition component analysis . *Journal of Electrical Technology* 31 (20): 41–54.